EUROfusion

WPJET1-PR(18) 21504

D Frigione et al.

Impact of Neon Injection on Electron Density Peaking in JET Hybrid Plasmas

Preprint of Paper to be submitted for publication in Nuclear Fusion

This work has been carried out within the framework of the EUROfusion Consortium and has received funding from the Euratom research and training programme 2014-2018 under grant agreement No 633053. The views and opinions expressed herein do not necessarily reflect those of the European Commission.

Impact of Neon Injection on Electron Density Peaking in JET Hybrid Plasmas

D. Frigione[1], M. Romanelli[2], C. Challis[2], J. Citrin[3], L. Frassinetti[4], E. Giovannozzi[1], J. Graves[5], J. Hobirk[6], F. Koechl[2], M. Mantsinen[7,8], M. Marin[3],C. Mazzotta[1], G. Pucella1, T. Putterich[6] and JET Contributors*

**See the author list of E. Joffrin et al 2018 IAEA FEC conference, India*

[1]ENEA, Fusion and Nuclear Safety Department, C. R. Frascati, Via E. Fermi 45, 00044 Frascati (Roma), IT, [2] CCFE, Culham Science Centre, OX143DB, UK, [3]FOM Institute DIFFER, Eindhoven, the Netherlands, [3] Association VR, Fusion Plasma Physics, KTH, SE-10044 Stockholm, Sweden, [4]EPFL, CRPP, 1015 Lausanne, Switzerland, [5]Max-Planck-Institut für Plasmaphysik, Boltzmannstr. 2, 85748 Garching, Germany, [6]ICREA, Barcelona, Spain, [7]Barcelona Supercomputing Center, Barcelona, Spain.

EUROfusion Consortium, JET, Culham Science Centre, Abingdon, OX14 3DB, UK

E-mail contact of main author: domenico.frigione@enea.it

Abstract. Impact of low-mid Z impurity injection on plasma transport and confinement has been observed and reported in several Tokamak experiments. Understanding particle transport in mixed species plasmas is crucial for reactor relevant conditions where control of DT mixture along with control of He concentration will be necessary. In this paper we present the analysis of experimental electron density profiles in JET hybrid scenario discharges with increasing level of neon seeding. The measured electron flux is compared with fully predictive transport simulations in search for the possible existence of a particle inward pinch proportional to the light impurity concentration as predicted by first principle gyro kinetic simulations. In preparation of full power operations (40 MW, 200 MJ) in DT experiments with Beryllium–Tungsten ITER-like first wall, neon was seeded into JET hybrid-scenario plasmas in order to increase the edge radiation and mitigate the divertor power loads. The average confinement performance was only slightly affected and neon injection turned out to be very effective in reducing the peak heat load at the strike points. However, in terms of fusion performance, neon doping caused a significant reduction of the neutron yield due to a number of effects originating from the peaking of the electron density profiles. The most relevant factor was the reduction of the central ion temperature, which, at the working point, could not be compensated by the corresponding local increase of the density or by increased ion heating. Although this effect will be less important in thermal fusion reaction dominated plasmas, it will remain relevant in JET DT experiments thus requiring further investigation.

1. Introduction

At present, there are no wall materials suitable to withstand the power loads predicted for burning tokamak plasmas while avoiding excessive tritium retention at the same time. Such solution is neither available for ITER nor even for full power DT experiments planned on JET. It is clear that finally most of the power will need to be exhausted via radiation, which has the advantage of spreading the power over a large area due to its intrinsic isotropy. Into the same direction of increasing the power wetted area, goes the so-called technique of 'sweeping' consisting in periodic radial displacement of the strike points. In order to favour peripheral radiation losses, impurity injection was considered and studied both theoretically and experimentally. In addition to the main purpose of exhausting power, our interest focused also on the impact of impurity seeding on density profiles and particle transport. This study could benefit from availability of high-resolution diagnostics and adequate modelling tools.

Impurity seeding was used on JET both in 'Baseline' and 'Hybrid' [1] scenarios for power exhaust mitigation purposes but only in Hybrid a systematic neon scan was performed at constant D2 fuelling. This gave the advantage of comparing shots with virtually the same parameters, including Deuterium fuelling, magnetic field, plasma current, q-profile shaping technique and wall conditioning. The only scanned parameter was the amount of injected neon. Some other hybrid shots, not belonging to this group, were added to better populate the scan area: in order to include them, the amount of injected neon was normalized to the D2 injection.

2. Database

The dedicated neon scan, consisting of 8 discharges, was performed at I_P = 1.4 MA, B_T = 1.9 T, β_N = 2.2 and Neutral Beam Injection power P_{NBI}=16.5 MW. Deuterium puffing waveform was kept constant during the scan while the neon was varied. Three of the above discharges had a small amount (< 1 MW) of Ion Cyclotron Resonance Heating (ICRH). The reason for not using more extensively ICRH power in spite of its ability to prevent impurity central accumulation was that the chosen magnetic field (1.9 T) was not optimised for central heating. The current ramp-up, overshooting the plateau value of 1.4 MA by 20% was used to produce a central $q_o \geq 1$ broad low shear region for NTM avoidance and because it may lead to better confinement [2]. Neon was injected at the start of the NBI heating phase and it was already present during the transition to H-mode: when the central density had reached its top value (≈ 4 s later) the Neon contribution to the total number of injected electrons ranged from 5% to 40%. Two un-seeded reference discharges were also performed during the same session with the same engineering parameters.

In order to populate the low/medium range of injected neon, other discharges from previous experiments have also been taken into account: in doing so, we normalised the total number of Neon injected electrons to Deuterium ones. Plasma current waveforms and toroidal field were the same as in the scan at constant D_2 flow rate. Figure 1 illustrates plasma current and Deuterium flow waveforms for the entire database.

Experimental density profiles were obtained from the High Resolution Thomson Scattering (HRTS) having 63 spatial detection points along one minor radius and a laser repetition rate of 20 Hz [3].

3. Experimental observations

Impact of low-mid Z impurity injection on plasma transport and confinement has been observed and reported in several Tokamak experiments [4,5]. At JET, the effect of neon injection on the divertor tile temperature, total energy confinement and neutron yield was already reported in ref. [6]. In brief, neon drives an increase of the volume averaged electron density, a reduction of the tile temperature and virtually no global confinement degradation. On the penalising side, a reduction of the neutron yield was observed (fig. 2): detailed analysis of the timing of the various mechanisms that can contribute to the neutron yield reduction (drop of T_i, dilution, beam penetration etc.) is in progress. However, preliminarily, it indicates that core T_i reduction could be the main cause, which was only partially compensated by the rise of the central particle density.

A close inspection of the electron density profiles has revealed a core peaking which increases with the amount of injected neon. Since we are mainly interested in the core particle confinement, we refer here to the peaking of the density profiles between the axis and the pedestal, discarding changes of the latter due to edge and SOL physics that we are not addressing in this paper. Figure 3 shows this effect by comparing two discharges with (#90280) and without neon (#90287). Neon injection causes also an increase of tungsten (W) influx likely due to sputtering from the W coated divertor tiles: the extra W tends to accumulate in the centre of the discharge as seen from spectroscopy analysis based on Soft X-ray emission according to ref. [7]. In absolute terms, the amount of observed tungsten can only give account of a fraction of the observed core electron density increment of the order of 0.1% as shown in fig.4. There we show the tungsten concentration multiplied by the local charge state (W_{el}), normalised to the observed electron density increase. An analysis of the peaking factor versus collisionality, using same definitions as in ref. [8], is shown in fig. 5. Two aspects are evident: a) neon seeded discharges reach higher peaking factors than those observed in the usual un-seeded case b) the enhanced peaking does not fall off with collisionality but, if anything, it would rather seem to stay constant or to weakly increase.

4. Interpretative hypothesis

In order to model the above discharges, fully predictive transport simulations of electron, deuterium and impurities densities and temperatures were carried out with JINTRAC [9] using Bohm-gyro-Bohm (BgB) transport coefficients, neoclassical collisional transport and calibrating the transport in the ETB region to reproduce the pedestal of the un-seeded reference pulse #90287. The target electron density is obtained via deuterium puff and 97% recycling. These settings are kept fixed in the predictive runs of seeded pulses with increasing neon concentration. It is found that using only BgB for the turbulent particle transport does not reproduce the observed increase of the electron density peaking with increasing neon concentration. Gyro-kinetic based models can qualitatively recover the effect of seeding on electron transport as preliminary seen by using QualiKiz. Nevertheless, for quantitative predictions, the model closure needs further development to take into account the physics of seeding.

The use of BgB allows to isolate and quantify the above effect via the addition of an ad-hoc particle pinch proportional to the effective charge (Z_{EFF}), representative of the neon concentration, and the ion temperature radial gradient $\partial_\rho T_i / T_i$:

$$V_e^{Ne}(r) = - C\, Z_{EFF}\, \partial_\rho T_i / T_i \quad \text{with } C = 0.1 \qquad (1)$$

In figure 6 and 7 we show the predicted electron density profiles in comparison with the HRTS data in the two sample cases of #90280 (seeded) and #90287 (un-seeded). In fig. 7 and 9 we do the same with temperature profiles.

The experimental pinch velocity can be calculated from the density profile change according to the following argument. Let Γ_e^{ref} be the particle flux through the pedestal (ρ=0.8) flux surface in the reference un-seeded pulse featuring a constant core density. Let also be S^{ref} be the total particle source within the plasma volume enclosed in the pedestal flux surface. Let this include the particle flux originated by the D puffing, the recycling and the one due to the NBI core deposition.

$$\nabla \cdot \Gamma_e^{ref} = S^{ref} \qquad (2)$$

When neon is added, the density increases with time, then we write the full particle balance equation including the density time derivative ($\partial_t n_e$), adding a particle flux (Γ_e^{Ne}) and a source (S_{Ne}) associated with neon injection.

$$\partial_t n_e + \nabla \cdot (\Gamma_e^{eq} + \Gamma_e^{Ne}) = S + S_{Ne} \qquad (3)$$

The additional source S_{Ne} is meant to include any additional particle source contributing to the increase of the pedestal density ($S_{Ne}=\partial_t n_{e-ped}$). The source inside the pedestal (S) is assumed to remain unchanged. Combining equation 2 and 3 we obtain:

$$\nabla\cdot\Gamma_e^{Ne} = -\partial_t n_e + \partial_t n_e(\rho=0.8) \quad (4)$$

Adopting the usual splitting of the particle flux in a diffusive term (D $\nabla\cdot V^{Ne}$) and a convective one ($n_e V_e^{Ne}$) and discarding the first one under the assumption that the turbulence is electrostatic we get $\Gamma_e^{Ne} = n_e\, V_e^{Ne}$ and consequently:

$$V_e^{Ne}\cdot\nabla n = -\partial_t\, n_e + \partial_t\, n_e(\rho=0.8) \quad (5)$$

And finally:

$$V_e^{Ne}(r) = [\, -\, \partial_t n_e(r) + \partial_t n_e(r=0.8)] \,/\, \partial_\rho n_e \quad (6)$$

The assumption of dealing with electrostatic turbulence only is justified by the relatively low beta in these plasmas and by the negligible population of fast particles due to the absence or the very tiny amount of ICRH power (< 1 MW).

The right hand side of equation (6) is evaluated from HRTS experimental density profiles according to the procedure described below. For each pulse we choose times t_1 and t_2 and plot the corresponding density profiles recording the values at centre $n_e(0,t_1)$, $n_e(0,t_2)$, and those at the pedestal $n_e(ped,t_1)$, $n_e(ped,t_2)$. Time t_1 is chosen as soon as the H-mode is well established in order to discard the initial density rise due to the transition to the high confinement mode; time t_2 is taken when the central density reaches its maximum. The nominator of equation 6 is evaluated as:

$$\{[n_e(0,t_2) - n_e(0,t_1)] - [n_e(ped,t_2) - n_e(ped,t_1)]\} \,/\, (t_2 - t_1) \quad [m^{-3}/\, s] \quad (7)$$

and the denominator as

$$[n_e(0,t_2) - n_e(ped,t_2)] \,/\, (R_{ped} - R_o) \;(8) \quad [m^{-3}/m] \quad (8)$$

(7) to (8) ratio correctly gives the pinch velocity in m/s.

Figure 10 compares the experimental particle pinches, at the same radial location, with the output of JETTO simulations, which include the effect of neon as, described above in this section. The abscissa is purely a measure of the amount of injected neon up to t_2 i.e. the time when the maximum peaking is reached. This quantity, calculated as number of electrons assuming that in the core Neon is fully ionised, is normalised to the D electrons injected up to the same time. This normalization is useful when considering also shots with different D puffing, which were added to populate the low/moderate seeding range (bottom box). Nevertheless, even without such an extension, JETTO simulations seem to reproduce correctly the experimental trend.

5. Conclusion

A neon scan was performed in Hybrid plasmas at JET in order to investigate the implications of using the impurity seeding technique for power exhaust mitigation purposes. The effect of neon on global performance was already reported in a previous paper and can be briefly summarised here: the technique was very efficient in reducing the divertor tile peak temperature without affecting the global confinement. Nevertheless, due to profile effects, the fusion performance represented by the total neutron yield was reduced. Here we analysed the impact of neon on the electron density profiles and the modification of the particle transport properties of the core plasma.

The experimental evidence was that the core electron density profiles featured a peaking effect increasing with the amount of injected neon. This was firstly observed at constant D fuelling but was also consistently observed in other plasmas when using, as scan parameter, the total amount of injected neon normalised to the injected deuterium. This additional peaking was not due to changes in collisionality nor it was possible to quantitatively attribute it to the observed W accumulation. According to soft X-rays spectroscopy, the contribution of W source of electrons was below 1% of the observed central density increment. On the diagram of peaking versus collisionality these pulses lied outside the familiar trend derived from un-seeded discharges. They featured a larger peaking factor for and no evident inverse trend with collisionality.

Modelling of different shots, with and without neon, showed that the observed peaking was well reproduced only if a particle pinch term, proportional to Z_{EFF} and grad T_i was introduced as predicted by ion temperature gradient driven theory (ITG).

Further experimental activity is planned to extend this study in the baseline scenario where a dedicated neon scan has not been performed yet.

References

1. Gruber O et al 1999 Phys. Rev. Lett. 83 1787J, Luce T C et al 2001 Nucl Fus 41 1585
2. Hobirk et al., Plasma Phys. Control. Fusion 54 (2012) 095001
3. R. Pasqualotto et al. Rev.Sci.Instr.,2004,vol.75,10
4. H. Urano et al. Nucl. Fusion 55 (2015) 033010
5. C. Mazzotta et al. Nucl. Fusion 55 (2015) 073027
6. C. Challis 44th EPS Conf. (2016) P2.153
7. T. Putterich et al. Plasma Phys. Control. Fusion 55 (2013) 124036
8. C. Angioni et al., Nucl. Fusion 47 (2007) 1326–1335
9. M. Romanelli et al, Plasma Fus. Res., Volume 9, 3403023 (2014)

Acknowledgments. This work has been carried out within the framework of the EUROfusion Consortium and has received funding from the Euratom research and training programme 2014-2018 under grant agreement No 633053. The views and opinions expressed herein do not necessarily reflect those of the European Commission.

FIGURES

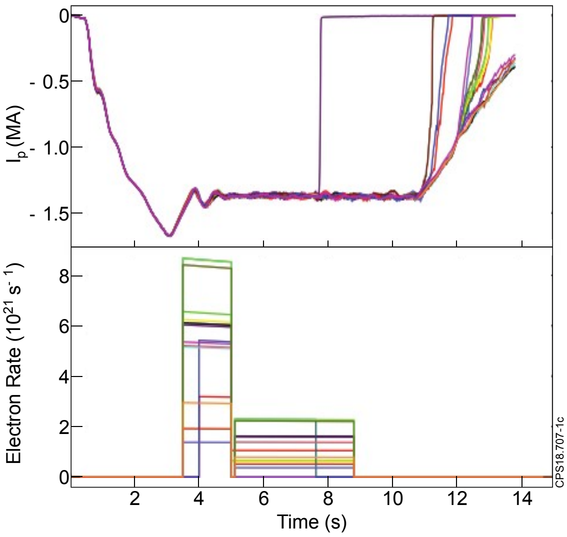

Fig. 1. Plasma current (top) and Neon electron flow rate (bottom) for all shots of the database. 1.4 MA, 1.9 T.

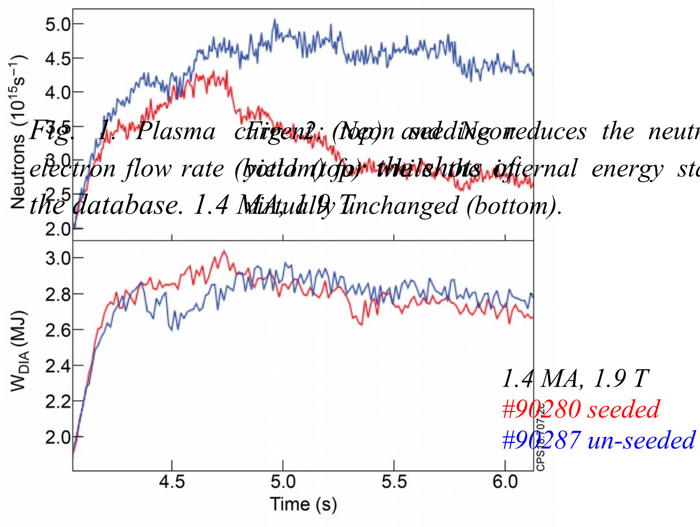

Figure 2: Neon seeding reduces the neutron yield (top) while the internal energy stays virtually unchanged (bottom).

W_{el}/ Δn_e

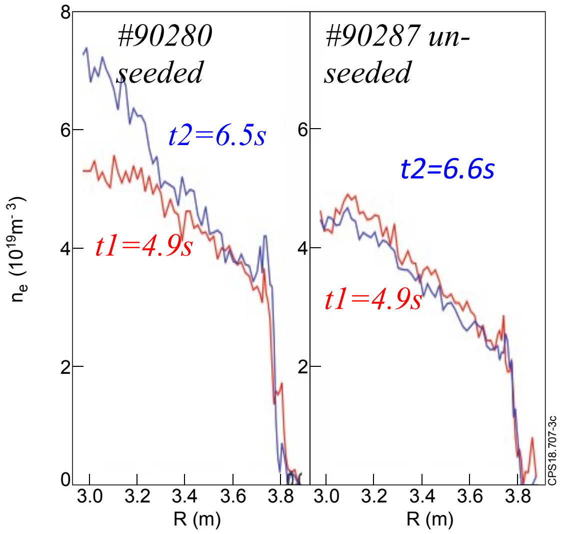

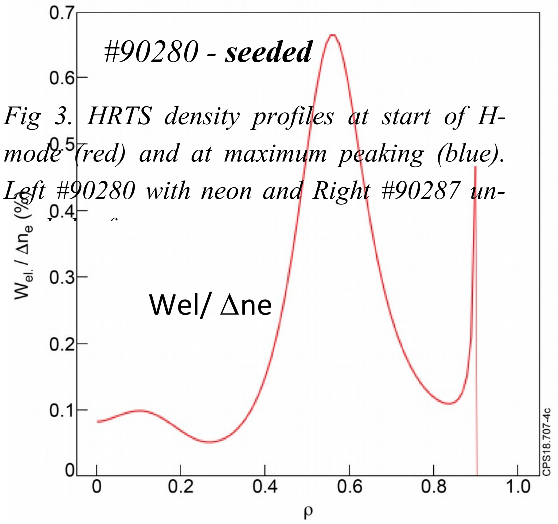

Fig 3. HRTS density profiles at start of H-mode (red) and at maximum peaking (blue). Left #90280 with neon and Right #90287 un-

Fig. 4. Profiles of electrons associated to tungsten (W_{el}) divided by extra density measured at t_2 with respect to t_1 ((Δn_e).

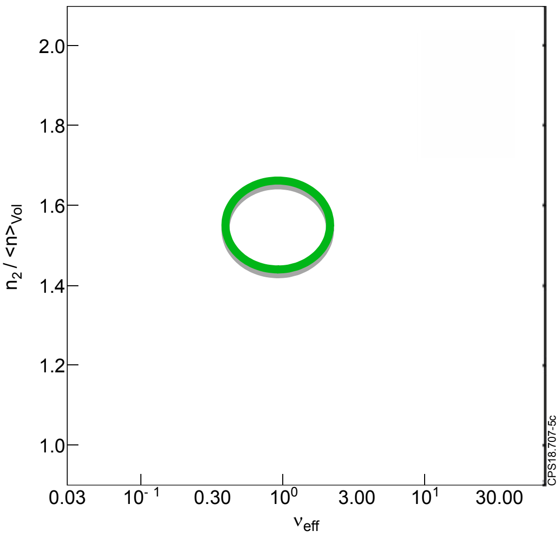

Fig. 5. *Peaking factor versus collisionality according to definitions given in ref. 8. Red diamond: neon seeding experiment presented here.. Other points reproduced from ref. 8 for un-seeded discharges. Points within the green circle have no or very low neon.*

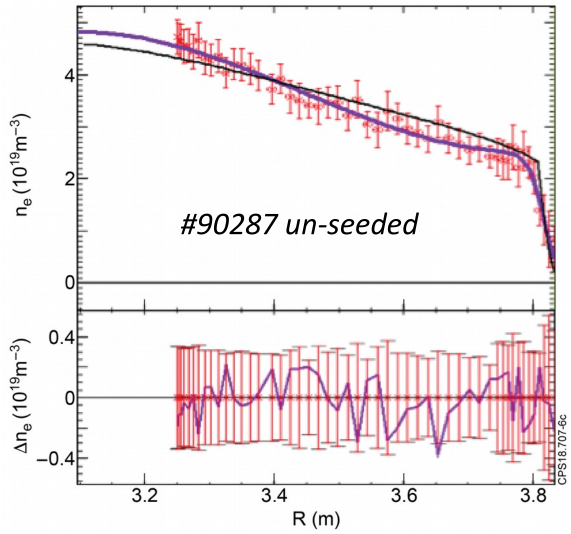

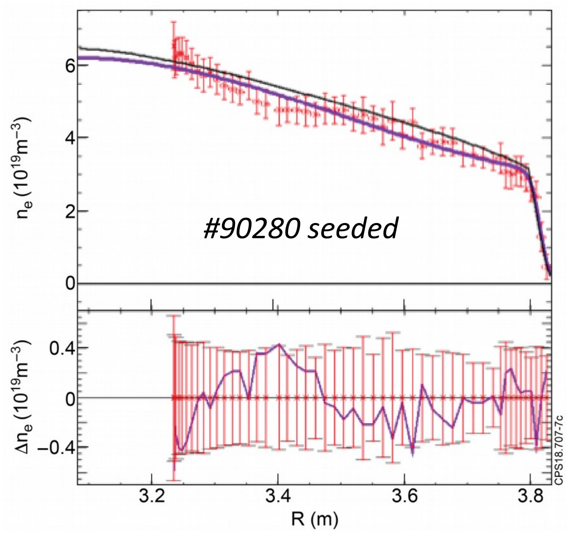

Fig. 6: electron density profiles @ t=6s of an un-seeded discharge (#90287). Green: simulation. Purple: fit of HRTS data. Bottom: difference between simulated and measured profiles with estimated experimental errors.

Fig. 7: electron density profiles @ t=6s of a seeded discharge (#90280.) Green: simulation. Purple: fit of HRTS data. Bottom: difference between simulated and measured profiles with estimated experimental errors.

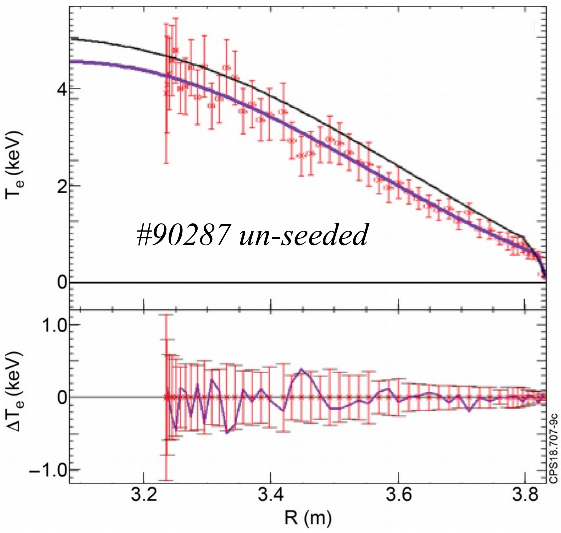

Fig. 8: electron temperature profiles @ t=6s of an un-seeded discharge (90287). Green: simulation. Purple: fit of HRTS data. Bottom: difference between simulated and measured profiles with estimated experimental errors.

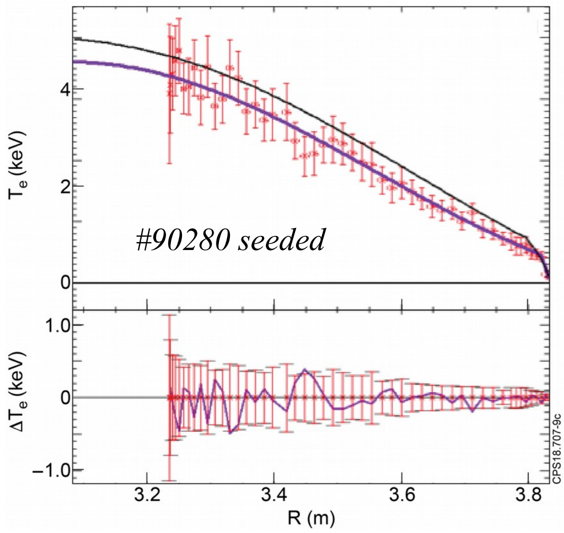

Fig. 9: electron temperature profiles @ t=6s of a seeded discharge (90287). Top: green/simulation. purple/ fit of HRTS data. Bottom: difference between simulated and measured profiles with estimated experimental errors.

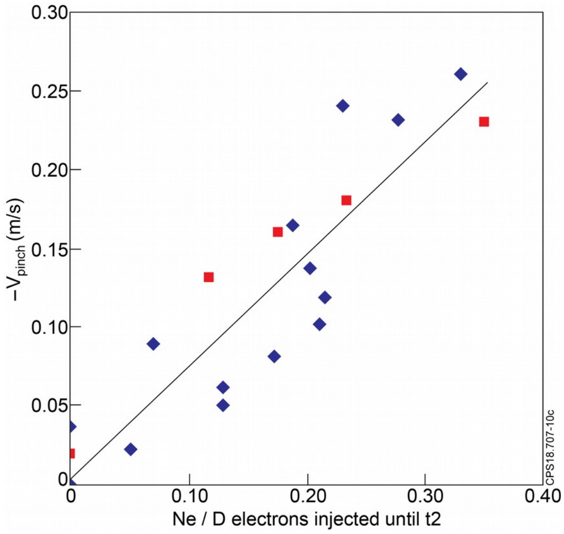

Fig. 10: Pinch velocity versus Ne/D electrons injected up to the time of maximum peaking (t_2).